

J. Wu

CSIRO, Division of Building, Construction
and Engineering,
Highett, Vic. 3190, Australia

J. Sheridan

Department of Mechanical Engineering,
Monash University,
Clayton, Vic. 3168, Australia

M. C. Welsh

CSIRO, Division of Building, Construction
and Engineering,
Highett, Vic. 3190, Australia

Velocity Perturbations Induced by the Longitudinal Vortices in a Cylinder Wake

This paper presents data showing the three-dimensional vortical structures in the near wake region of circular cylinders. The in-plane velocity field was measured using a digital Particle Image Velocimetry (PIV) technique. The vortical structures are found to include inclined counter-rotating longitudinal vortices in the braids joining consecutive Kármán vortices. A simple vortex-pair model is proposed to estimate velocity perturbation induced by the longitudinal vortices in the near wake region. The perturbation resulting from the longitudinal vortices is shown to induce spanwise velocity modulation and a velocity spike of a nominally two-dimensional vortex street.

Introduction

It has been recognised in recent years that the wake of a bluff body develops three-dimensional vortical structures. Williamson (1988), Williamson et al. (1995), Wei and Smith (1986), Welsh et al. (1992), Bays-Muchmore and Ahmed (1993), and Wu et al. (1994a, 1994b, 1996) have all shown that the three-dimensional vortical structures include inclined pairs of counter-rotating longitudinal vortices, having streamwise and transverse vorticity components. They form rib-like structures in the braids joining successive Kármán vortices. Similar three-dimensional vortical structures were shown to exist in plane mixing layers by Bernal and Roshko (1986), among others.

The development of three-dimensional instabilities and the formation of small-scale longitudinal vortices are related to local turbulence production and fine-scale velocity fluctuations (Hussain, 1986; Ferre et al., 1990) in turbulent wake flows. An understanding of the fluid dynamics involved is of great interest to fluid mechanics in general and in particular to engineering technologies and computational fluid dynamics.

Wu et al. (1994b) showed, using a digital PIV technique, that the vorticity of longitudinal vortices is twice that of the Kármán vortices upon which the former are superimposed. This is consistent with the theory of Meiburg and Lasheras (1988) that the longitudinal vortices are being stretched by the spanwise vortices (i.e., Kármán vortices). This strong vorticity field induced by the longitudinal vortices could be significant in the development of the Kármán vortex street. The present work sought to explore this further by quantifying the velocity perturbation induced in the wake by the longitudinal vortices.

In this paper, the same digital PIV technique (Wu et al. 1994b) was used to obtain instantaneous in-plane velocity distributions in the wake of a circular cylinder. Quantitative information of the strength of the longitudinal vortices and their influence on the velocity distributions were obtained. The data obtained make it possible to analyse the velocity perturbation resulting from the longitudinal vortices, and to develop a simple model that can predict the amplitude of the spanwise velocity modulation and the magnitude of apparent velocity spikes.

It will be shown that the spanwise velocity modulation can be as large as two thirds of the freestream velocity, due to the perturbation of the longitudinal vortices. Spanwise velocity profiles of wakes are rarely reported, partly because of the diffi-

culty of capturing three-dimensional features using conventional single-point probes and partly because of the lack of understanding of flow three-dimensionalities. There has, however, been some success in using single sensors to measure the time-mean spanwise velocity profile in mixing layer investigations. Huang and Ho (1990) studied the small-scale transition process of a mixing layer using an X-wire probe. They measured the spanwise distribution of the time-mean streamwise velocity profile. The profiles contained clear wavy patterns, which they pointed out were due to the formation of streamwise vortices (longitudinal vortices). The amplitude of the wavy pattern varies from $0.1\bar{U}$ to $0.2\bar{U}$ (\bar{U} is the average velocity of the mixing layer), depending on streamwise distance.

Experimental Arrangement and Facilities

Water Tunnel and Test Models. A return-circuit water tunnel schematically shown in Fig. 1 was used for the experiments. Water was pumped into a settling chamber containing filters and a honeycomb and then passed through a 4:1 contraction before entering the working section. The water leaving the working section flowed via a 440 mm long duct into an outlet reservoir tank. The working section is 770 mm long with a cross-section of 244 by 244 mm. The walls are transparent, being made of acrylic.

Circular cylinders used in these experiments were made of 244 mm long polished plexiglass with diameters of 3.3, 6.4 and 9.4 mm. End-plates were used to reduce the possible interference of the boundary layer forming along the test section walls. The freestream velocity was uniform to within 1 percent outside the boundary layers and the longitudinal turbulence level was typically 0.1 percent when band-pass filtered between 0.08 and 20 Hz. No clear spectral spikes were evident in the longitudinal velocity signal.

PIV Technique. Flow was seeded with hollow microsphere beads with a mean diameter $< 30 \mu\text{m}$. An 8W argon-ion continuous laser beam was transmitted through a $50 \mu\text{m}$ diameter multi-mode optical fibre and spread into a light sheet using a cylindrical lens. The light scattered from the particles in the laser sheet was recorded using a "Videk" digital CCD camera with a spatial resolution of 1280×1024 pixels; the light intensity signal was digitised into 256 levels (8-bit) on a personal computer. Single-frame, multiply-exposed particle images were sampled and processed using software based on the Young's fringe method to give the in-plane velocity distribution. The words in-plane will be used in the paper to refer to the two-

Contributed by the Fluids Engineering Division for publication in the JOURNAL OF FLUIDS ENGINEERING. Manuscript received by the Fluids Engineering Division April 5, 1995; revised manuscript received April 15, 1996. Associate Technical Editor: M. Gharib.

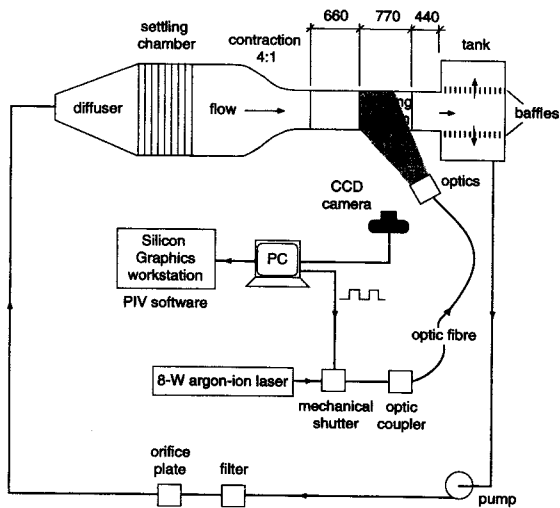


Fig. 1 Experimental setup

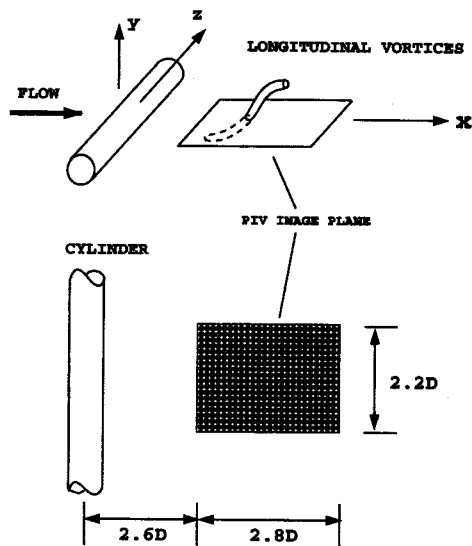


Fig. 2 The PIV image plane was in the centerline plane of the cylinder and $2D$ behind the back of the cylinder. The image size was $2.8 \times 2.2D$.

dimensional plane where the PIV measurement was conducted to give two velocity components in that plane. The principle of the PIV technique was outlined in the early work of Barker and Fournay (1977). Excellent reviews are available on PIV techniques, and readers are referred to Adrian (1991) and Buchhave (1992). In the present application, the Young's fringe pattern was found by performing FFT calculations on a Silicon Graphics workstation and an algorithm was used to calculate the spacing and orientation of the fringe patterns to determine the velocity vectors.

Nomenclature

d = vortex core diameter (mm)
 D = diameter of cylinder (mm)
 Re = Reynolds number based on D and U_0 (non.)
 U_0 = freestream velocity (m/s)
 u, w = streamwise and spanwise flow velocity (m/s)

u_{max} = maximum of spanwise profile of u (m/s)
 u'_{max} = the amplitude of velocity spike (m/s)
 \bar{u} = spanwise average of u (m/s)
 x, y = streamwise and transverse coordinate, zero at cylinder center (mm)
 z = spanwise coordinate (mm)

δu_{max} = the amplitude of spanwise modulation of u (m/s)
 δw_{max} = the amplitude of variation of w (m/s)
 Γ = circulation of a longitudinal vortex (m^2/s)
 ω_y = y -direction vorticity component, normal to the measurement plane (1/s)

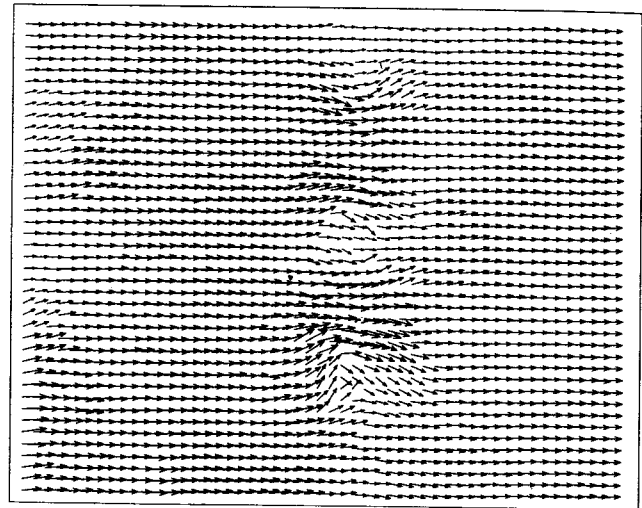


Fig. 3(a)

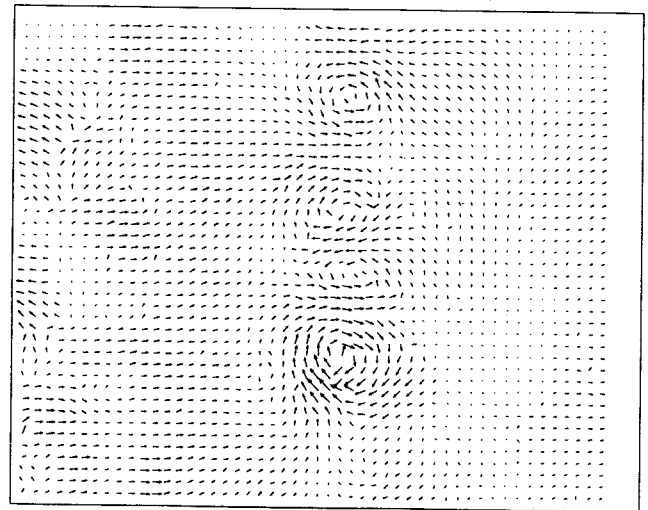


Fig. 3(b)

Fig. 3 Velocity vector field with frame of reference (a) fixed to the cylinder, (b) moving with the vortices at 60 percent U_0 . The velocity grid resolution was 0.5 mm, $D = 9.4$ mm, $Re = 550$.

The uncertainty of the velocity measurement is 4 percent at a confidence level of 95 percent. The uncertainty of circulation is equal to that of the velocity measurements.

Results

Overview. The experiments were conducted at Reynolds numbers ranging from 140 to 550. Because of the limited space, data will be presented only for $Re = 550$, which is well above

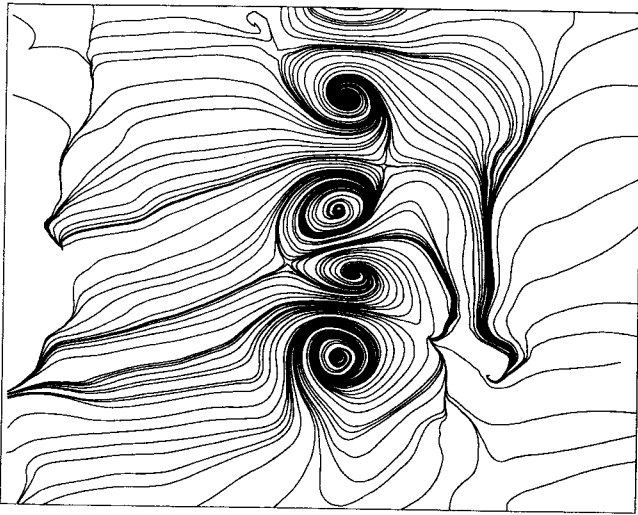


Fig. 4(a)

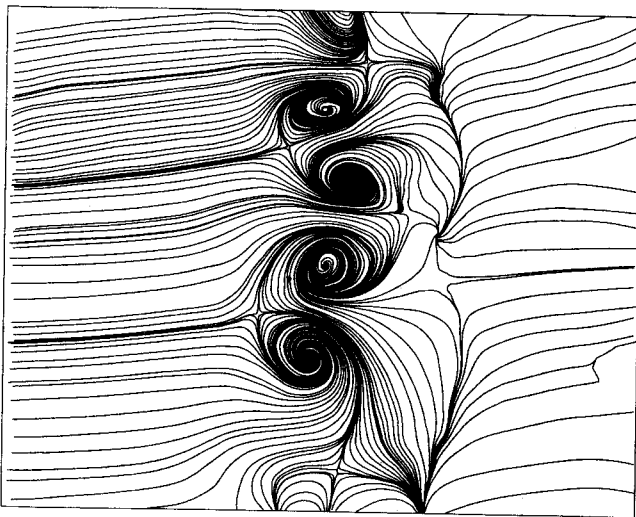


Fig. 4(b)

Fig. 4 Typical streamline patterns at two arbitrary instants, sampled randomly in time at $Re = 550$ (the streamlines here are not drawn at constant intervals)

the transitional range for the onset of the three-dimensional vortices (occurs at $Re \approx 175$, Williamson (1988) and Wu et al. (1994a)).

Instantaneous in-plane velocity distributions were measured in a transverse plane located $2D$ behind the back of the cylinder and in a plane passing through the cylinder centre-line, as shown in Fig. 2. The measurement plane was chosen to cut across the inclined longitudinal vortices joining consecutive Karman vortices in the wake. The measurement plane covered an area of $2.8D$ in the streamwise and $2.2D$ in the spanwise directions. A typical velocity vector field, showing flows in the transverse plane, is presented in Figs 3(a) and (b) at $Re = 550$. The frame of reference in Fig. 3(a) is fixed to the cylinder while in Fig. 3(b) it moves with the vortices. Pairs of vortices can be seen to be spinning in opposite directions along the cylinder span.

Two typical instantaneous streamline patterns, as calculated from the velocity data, are shown in Fig. 4, in a frame of reference moving with the vortices. The counter-rotating longitudinal vortices, being intersected by the measurement plane, are evident as the mushroom-type structures. As an interesting comparison, readers are referred to the hydrogen-bubble flow

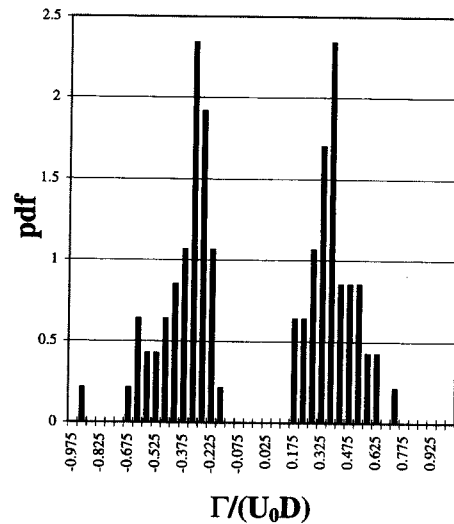


Fig. 5 Probability density function distribution of circulation of longitudinal vortices at $Re = 550$, the data are normalized by U_0 and D , the number of samples is 50

patterns presented by Wei and Smith (1986) and Wu et al. (1994a).

Spanwise Velocity Modulation. Clearly, the action of longitudinal vortices will distort the velocity field of a vortex street resulting in spanwise velocity modulation. The extent of this distortion can be quantified from the PIV measurements.

To do this, the circulation of a longitudinal vortex has been estimated by integrating vorticity over the area in which the vorticity ω_y is greater than 10 percent of $\omega_{y,max}$, where ω_y is the vorticity perpendicular to the measurement plane and $\omega_{y,max}$ is the maximum vorticity perpendicular to the measurement plane. It should be pointed out that the circulation obtained in the current measurement plane represents the circulation of the inclined longitudinal vortices, as the circulation along a closed line surrounding a vortex is independent of the way the line is drawn. A typical probability density function distribution (or histogram) of measured circulation of longitudinal vortices, is plotted in Fig. 5 for $Re = 550$. This has been calculated from 50 frames of randomly sampled particle images. Clearly the strength of the positive and the negative vorticity in the two

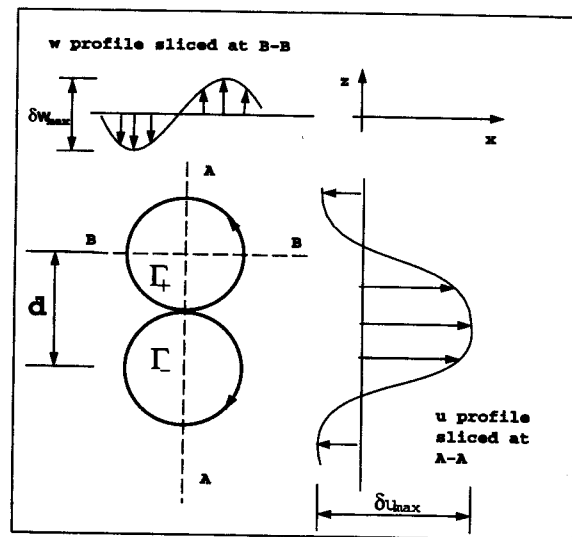


Fig. 6 A simple velocity perturbation model, flow induced by a pair of ideal Rankine-vortex

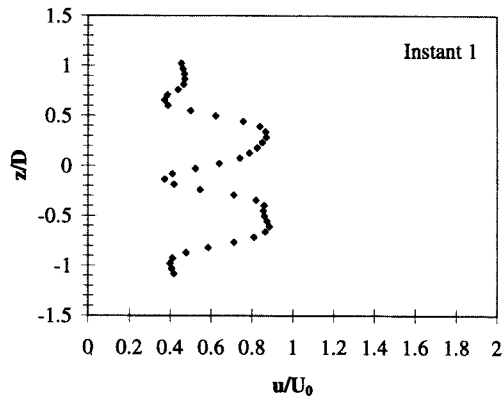


Fig. 7(a)

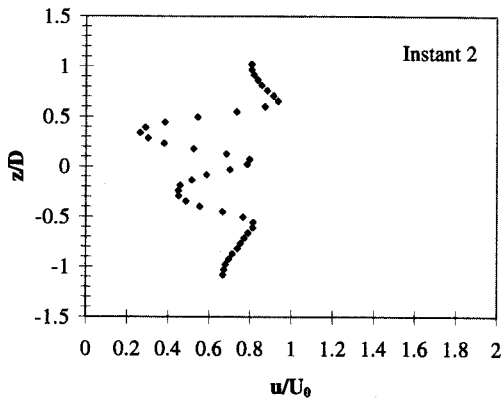


Fig. 7(b)

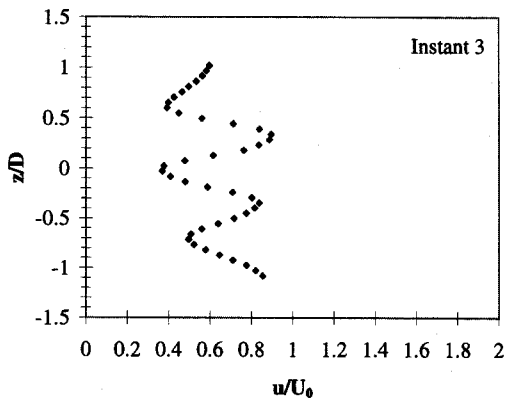


Fig. 7(c)

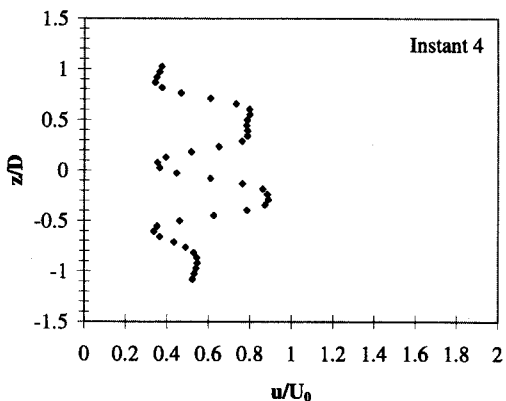


Fig. 7(d)

Fig. 7 Velocity spanwise modulation at 4 arbitrary instants, streamwise velocity component u variation along cylinder span, the instantaneous data were sampled randomly at $Re = 550$.

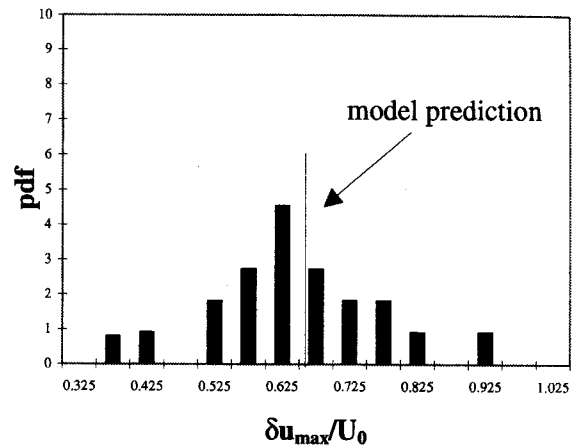


Fig. 8 Probability density function of the velocity modulation amplitude at $Re = 550$

parts of a vortex pair is statistically balanced, as is expected. The mean circulation can be expressed as:

$$\Gamma \approx 0.39U_0D \quad (1)$$

where U_0 is the freestream velocity and D is the cylinder diameter. Measurements performed for a range of Reynolds numbers reveal that this correlation is valid when the Reynolds number is well above a transitional range, i.e., $Re > 250 \sim 300$.

Now that the circulation of the longitudinal vortices is known, the induced spanwise velocity modulation can be estimated by considering an ideal vortex pair in the $x-z$ plane, as schematically shown in Fig. 6, where the z -axis corresponds to the cylinder axis (spanwise direction). The parameter δu_{max} shown in the figure is used to characterise the level of velocity spanwise modulation. Based on the above ideal vortex pair model, it is elementary to show:

$$\delta u_{max} \approx \frac{2.67\Gamma}{\pi d} \quad (2)$$

where d is the average vortex core diameter. Substituting the correlation for Γ in (1), we get:

$$\delta u_{max} \approx 0.33 \frac{U_0D}{d} \quad (3)$$

The vortex core diameter is found to be $d \approx 0.5 D$, which is approximately half of the spanwise wavelength of the vortices (the spanwise wavelength of the vortices has been found to be approximately equal to one cylinder diameter by Williamson

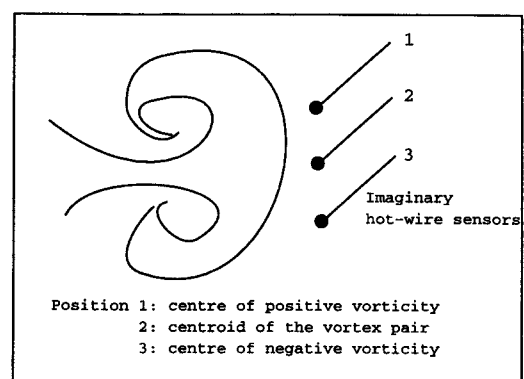


Fig. 9 Places of an imaginary hot-wire probe, No. 1: aligned to the center of the positive vorticity, No. 2: aligned to the centroid of the vortex pair, No. 3: aligned to the centre of the negative vorticity

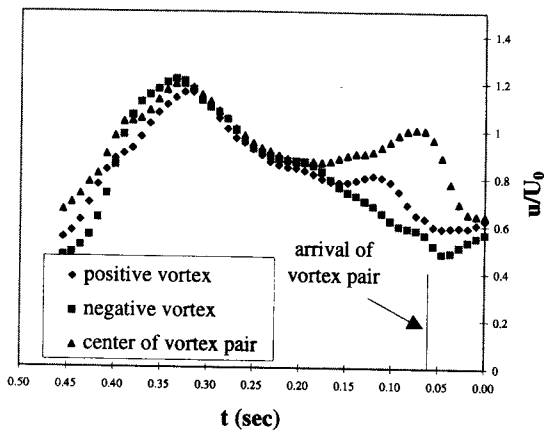


Fig. 10(a)

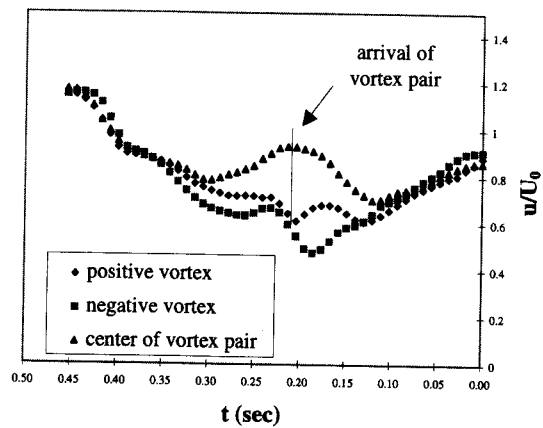


Fig. 10(b)

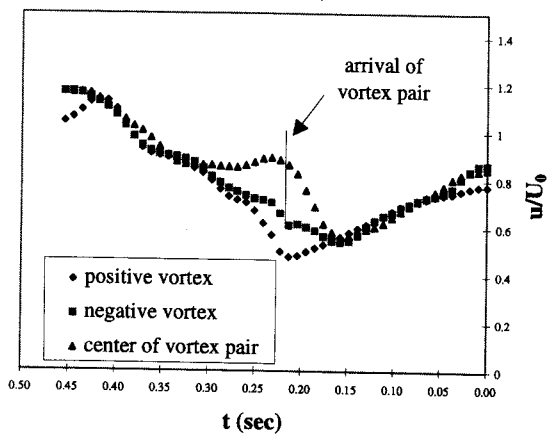


Fig. 10(c)

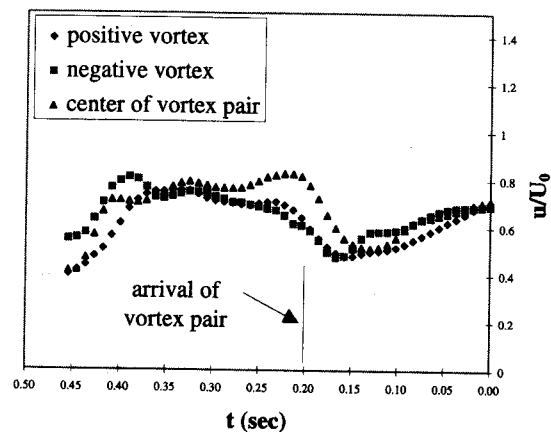


Fig. 10(d)

Fig. 10 Temporal velocity fluctuation obtained by invoking Taylor's hypothesis. The three curves correspond to the probe being at the centre of the positive vortex (vorticity), at the centre of the negative vortex (vorticity) and at the centroid of a vortex pair, respectively, the convective velocity used for transform is $0.8U_0$. The data were sampled at 4 arbitrary instants.

(1988), Bays-Muchmore and Ahmed (1993), and Wu et al. (1994a)). The amplitude of the spanwise velocity modulation can therefore be estimated as below, where $d = 0.5D$ is used:

$$\delta u_{max} \approx 0.66U_0 \quad (4)$$

Typical spanwise modulations of the streamwise velocity component, u , sliced through the centres of pairs of longitudinal vortices, are plotted in Fig. 7 at four instants. It should be noted that the spanwise variation of u/U_0 is dependent on the streamwise location where the measurement is made. As the u/U_0 velocity profiles in Fig. 7 are all taken slicing through the centres of the longitudinal vortices they represent the maximum influence produced. On the other hand, the influence of the spanwise vortices is to produce a background velocity variation in the streamwise direction, this becomes clear when a streamwise slice of the measurement plane is plotted as shown later in Fig. 10. The probability density function distribution of the modulation amplitude δu_{max} has been calculated and the result is shown in Fig. 8. The prediction based on the forementioned model is also indicated in the figure and there is reasonable agreement between the model and the data.

In passing, it should be noted that it is also possible to provide information on the induced spanwise velocity component w . In a similar fashion, a parameter δw_{max} is defined in Fig. 6 to characterize the induced spanwise velocity component. In this case, the meaningful velocity profile is taken from a slice (e.g., B-B in Fig. 6) through the centre of the one of the two vortices. The result based on the present PIV measurement is:

$$\delta w_{max} \approx 0.41U_0 \quad (5)$$

Velocity Spike. Imagine if an Eulerian probe (e.g., a hot-wire probe or a LDA) were placed in a bluff body wake to measure the velocity variation with time. Velocity fluctuations caused by the longitudinal vortices would be sensed by the probe if it were placed at the right position at the right time. With instantaneous velocity data measured using the PIV technique, it is possible to "animate" such an event. Taylor's frozen flow hypothesis is assumed to be valid for a very short period of time, during which the flow structures containing the vortices are to be convected downstream unchanged and at the convective velocity of the vortex street. This transformation is expressed as:

$$f(x) = f(U_c t) \quad (6)$$

where x and t are spatial and temporal coordinates, $f(x)$ is the spatial distribution of a certain fluid quantity, U_c is the convection velocity, and $f(U_c t)$ is the temporal distribution derived from $f(x)$.

Typical velocity time evolution signals as seen by the imaginary stationary probes placed at the centre of a positive vortex (i.e., with positive vorticity), the center of a negative vortex and the centroid of the vortex pair as shown in Fig. 9 are plotted in Figs 10(a), (b), (c), and (d) where time increases from right to left corresponding to flow from left to right. The arrival of a vortex pair in time is indicated by the vertical dotted lines, calculated from the spatial position of the centroid of the vortex pairs. A velocity spike clearly emerges at the time of arrival of vortex pairs and the fluctuation is maximum when the "probe" is located at the centroid of a vortex pair. It is seen that the

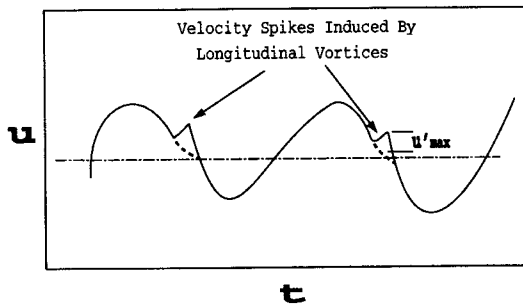


Fig. 11 Conceptual diagram on the effect of generation of velocity spikes due to the action of the longitudinal vortices in a cylinder wake

amplitude of the velocity spike is very sensitive to where the 'probe' is placed. The amplitude reduces substantially when the probe is shifted away from the centroid of a vortex pair.

In summary, in addition to the pure periodic velocity oscillation expected to be detected by a hot-wire (or LDA) probe placed in the wake of a bluff body, spikes, as illustrated in Fig. 11, should exist in the time velocity fluctuation signal of a three-dimensional vortex street behind a bluff body. It is useful to estimate the amplitude of the velocity spikes, u'_{max} , as defined in Fig. 11. An estimation of u'_{max} can be made from the spanwise variation of the streamwise velocity component (shown in Fig. 7):

$$u'_{max} = u_{max} - \bar{u} \approx \delta u_{max}/2 \quad (7)$$

where u_{max} and \bar{u} represent the maximum and the spanwise average of u component, respectively. Using the previous results, it is concluded that $u'_{max} \approx 0.33U_0$. The prediction is in reasonable agreement with the measurements (see, for example, the data in Fig. 10).

Concluding Remarks

A digital Particle Image Velocimetry (PIV) technique has been used to measure the velocity field in the wake of circular cylinders. The instantaneous in-plane velocity distributions obtained in a plane parallel to the cylinder axis reveal the perturbations to the flow induced by the inclined longitudinal vortices. Pairs of these vortices along the cylinder span have been shown to produce the mushroom-type structures in the streamline patterns. Spanwise instantaneous velocity modulations generated by the longitudinal vortices are presented. A simple vortex-pair model is suggested to predict the modulation amplitude and is found to agree well with the measurements. The mechanisms of velocity spikes are illustrated by using Taylor's hypothesis, together with data and correlation for their characterisation.

The velocity spikes caused by the longitudinal vortices contribute to an increase in high frequency components in the flow's kinetic energy spectrum. The amplitude of these spikes can be estimated when the strengths of the longitudinal vortices are known. The present paper provides a way to predict the amplitude of the spikes. It is recognised that in a real situation, the longitudinal vortices are not located in a fixed spanwise position (Wu et al., 1994a), instead they are being generated randomly across the cylinder span. The velocity fluctuations associated with the velocity spikes may look irregular for a stationary probe.

Acknowledgment

J. Wu and J. Sheridan acknowledge the support from an Australian Research Council grant. The authors wish to thank R. F. La Fontaine and L. Welch for many helpful discussions and technical assistance during the experiments.

References

- Adrian, R. J., 1991, "Particle Imaging Techniques for Experimental Fluid Mechanics," *Annual Review of Fluid Mechanics*, Vol. 23, pp. 261-304.
- Barker, D. B., and Fourny, M. E., 1977, "Measuring Fluid Velocities with Speckle Patterns," *Optics Letters*, Vol. 1, No. 4, pp. 135-137.
- Bays-Muchmore, B., and Ahmed, A., 1993, "On Streamwise Vortices in Turbulent Wakes of Cylinders," *Physics of Fluids A*, Vol. 5, No. 2, pp. 387-392.
- Bernal, L. P., and Roshko, A., 1986, "Streamwise Vortex Structure in Plane Mixing Layers," *Journal of Fluid Mechanics*, Vol. 170, pp. 499-525.
- Buchhave, P., 1992, "Particle Image Velocimetry—Status and Trends," *Experimental Thermal and Fluid Science*, Vol. 5, pp. 586-604.
- Ferre, J. A., Mumford, J. C., Savill, A. M., and Ciralt, F., 1990, "Three-dimensional Large-eddy Motions and Fine-scale Activity in a Plane Wake," *Journal of Fluid Mechanics*, Vol. 210, pp. 371-414.
- Huang, Lein-Saing, and Ho, Chih-Ming, 1990, "Small-scale Transition in a Plane Mixing Layer," *Journal of Fluid Mechanics*, Vol. 210, pp. 475-500.
- Hussain, A. K. M. Fazle, 1986, "Coherent Structures and Turbulence," *Journal of Fluid Mechanics*, Vol. 173, pp. 303-356.
- Meiburg, E., and Lasheras, J. C., 1988, "Experimental and Numerical Investigation of the Three-dimensional Transition in Plane Wakes," *Journal of Fluid Mechanics*, Vol. 190, pp. 1-37.
- Wei, T., and Smith, C. R., 1986, "Secondary Vortices in the Wake of Circular Cylinders," *Journal of Fluid Mechanics*, Vol. 169, pp. 513-533.
- Welsh, M. C., Soria, J., Sheridan, J., Wu, J., Hourigan, K., and Hamilton, N., 1992, "Three-dimensional Flows in the Wake of a Circular Cylinder," *Album of Visualization, The Visualization Society of Japan*, Vol. 9, pp. 17-18.
- Williamson, C. H. K., 1988, "The Existence of Two Stages in the Transition to Three-dimensionality of a Cylinder Wake," *Physics of Fluids*, Vol. 31, No. 11, pp. 3165-3168.
- Williamson, C. H. K., Wu, J., and Sheridan, J., 1995, "Scaling of streamwise vortices in wakes," *Physics of Fluids*, Vol. 7, No. 10, pp. 2307-2309.
- Wu, J., Sheridan, J., Soria, J., and Welsh, M. C., 1994a, "An Experimental Investigation of Streamwise Vortices in the Wake of a Bluff Body," *Journal of Fluids & Structures*, Vol. 8, pp. 621-635.
- Wu, J., Sheridan, J., Welsh, M. C., Hourigan, K., and Thompson, M., 1994b, "Longitudinal Vortex Structures in a Cylinder Wake," *Physics of Fluids*, Vol. 6, No. 9, pp. 2883-2885.
- Wu, J., Sheridan, J., Welsh, M. C., and Hourigan, K., 1996, "Three-dimensional Vortex Structures in a Cylinder Wake," *Journal of Fluid Mechanics*, Vol. 312, pp. 201-222.